AD-A081 185 VARIAN ASSOCIATES PALO ALTO CA SOLID STATE LAB F/G 9/5
III-V HETEROSTRUCTURE AVALANCHE PHOTODIODE MODULES FOR FIBER OP--ETC(U)
SEP 79 R YEATS DAAB07-78-C-2402
UNCLASSIFIED NL

1 OF 1
AD-
A081185

END
DATE
FILMED
3-80
DDC

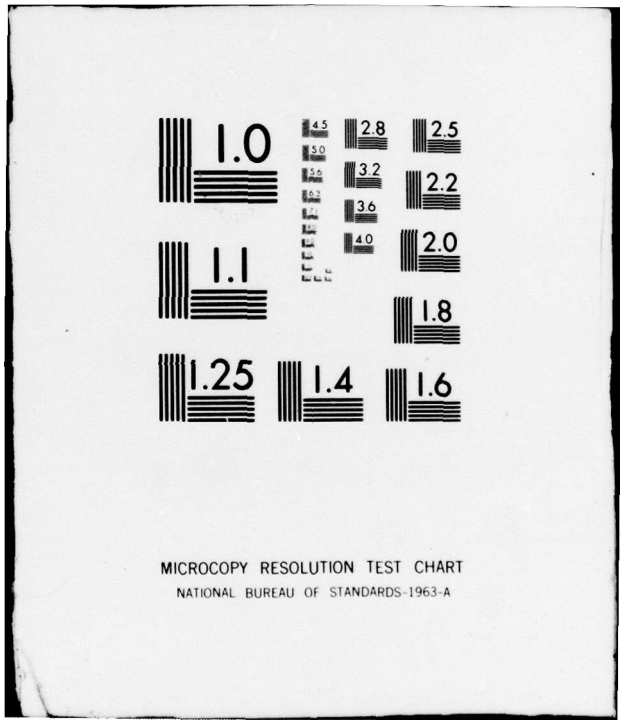
1.0
1.1
1.25
1.4
1.6
1.8
2.0
2.2
2.5
2.8
3.2
3.6
4.0
4.5
5.0
5.6
6.3
7.1
MICROCOPY RESOLUTION TEST CHART
NATIONAL BUREAU OF STANDARDS-1963-A

LEVEL II

III-V HETEROSTRUCTURE AVALANCHE PHOTODIODE MODULES FOR FIBER OPTIC COMMUNICATION LINKS IN THE 1.0 TO 1.3 MICROMETER SPECTRAL RANGE

INTERIM REPORT NO. 3

(February 1979 - July 1979)

September 1979

Prepared for:

U.S. Army Communication R&D Command
Fort Monmouth, New Jersey 07703

Contract No. DAAB07-78-C-2402

Prepared by:

R. Yeats

Solid State Laboratory
Varian Associates, Inc.
611 Hansen Way
Palo Alto, CA 94303

UNCLASSIFIED
SECURITY CLASSIFICATION OF THIS PAGE (When Data Entered)

REPORT DOCUMENTATION PAGE

READ INSTRUCTIONS BEFORE COMPLETING FORM

1. REPORT NUMBER: Interim Report No. 3	2. GOVT ACCESSION NO.: -
3. RECIPIENT'S CATALOG NUMBER: --	
4. TITLE (and Subtitle): III-V Heterostructure Avalanche Photodiode Modules for Fiber Optic Communication Links in the 1.0 to 1.3 Micrometer Spectral Range	5. TYPE OF REPORT & PERIOD COVERED: Technical Report (Feb -July 1979)
	6. PERFORMING ORG. REPORT NUMBER: -
7. AUTHOR(s): R. Yeats	8. CONTRACT OR GRANT NUMBER(s): DAAB07-78-C-2402
9. PERFORMING ORGANIZATION NAME AND ADDRESS: Varian Associates, Inc. 611 Hansen Way Palo Alto, CA 94303	10. PROGRAM ELEMENT, PROJECT, TASK AREA & WORK UNIT NUMBERS: 12 29 -
11. CONTROLLING OFFICE NAME AND ADDRESS: U.S. Army Communication R&D Command Fort Monmouth, NJ 07703 (C. Loscoe)	12. REPORT DATE: September 1979
	13. NUMBER OF PAGES: 19
14. MONITORING AGENCY NAME & ADDRESS (if different from Controlling Office)	15. SECURITY CLASS. (of this report): Unclassified
	15a. DECLASSIFICATION/ DOWNGRADING SCHEDULE

16. DISTRIBUTION STATEMENT (of this Report)

Interim rept. no. 3, Feb-Jul 79,

17. DISTRIBUTION STATEMENT (of the abstract entered in Block 20, if different from Report)

18. SUPPLEMENTARY NOTES

19. KEY WORDS (Continue on reverse side if necessary and identify by block number)

indium gallium arsenide phosphide photodiode
indium gallium arsenide
indium phosphide
avalanche photodiode

20. ABSTRACT (Continue on reverse side if necessary and identify by block number)

The increased leakage current in InGaAsP APDs near breakdown is found to be a rather uniform bulk property, not associated with conventional microplasmas, dislocations, or surface effects. Surface effects were eliminated by the fabrication of guard ring APDs, but the increased leakage current persisted. Surface effects were further ruled out by a statistical study of a large sample of APDs, which showed conclusively that the APD leakage current is proportional to diode area, not perimeter. Attempts to overcome the

Next page

DD FORM 1 JAN 73 1473 EDITION OF 1 NOV 65 IS OBSOLETE

UNCLASSIFIED
SECURITY CLASSIFICATION OF THIS PAGE (When Data Entered)

20. ABSTRACT (Cont.)

leakage current problem are still being made.

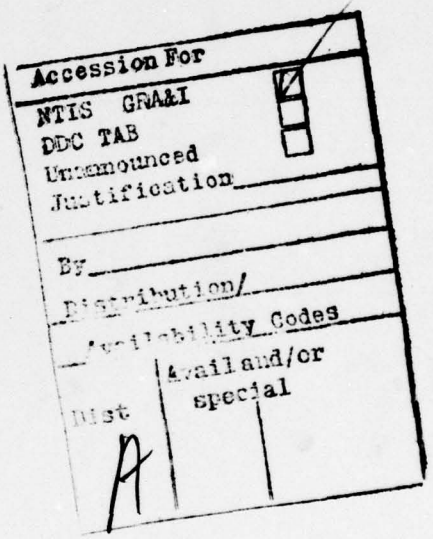

SUMMARY

While InGaAsP APDs are superb as photodiodes, with low leakage current, subnanosecond speed, and nearly 100% internal quantum efficiency, their performance as APDs has been limited. Due to a large increase in leakage current in the avalanche gain region of bias, useful gains have been small, even though moderately large uniform gains are available. In the present work, the increased leakage current in InGaAsP APDs near breakdown is found to be a rather uniform bulk property, not associated with conventional microplasmas, dislocations, or surface effects. Surface effects were eliminated by the fabrication of guard ring APDs, but the increased leakage current persisted. Surface effects were further ruled out by a statistical study of the leakage current in a large sample of APDs. The study shows conclusively that the leakage current is proportional to diode area, not perimeter. While the nature of the increased leakage current has been clarified, its cause is still unknown. Attempts to solve or circumvent the leakage current problem are still being made.

PREFACE

The work reported here was supported by the U.S. Army Communications R&D Command, Fort Monmouth, New Jersey, under Contract DAAB07-78-C-2402. The CORADCOM project engineer is Ms. Claire Loscoe. The program is aimed at the development of high-performance III-V avalanche photodiodes for detection in the 1.0 to 1.3-micron wavelength range.

The work was carried out in the Varian Corporate Research Solid State Laboratory. Major contributions to this work were made by R. Yeats and S. H. Chiao.* Assistance was also provided by G. A. Antypas, S. B. Hyder, R. L. Bell, C. Hooper and K. Van Dessonneck.

---

*Present Address: Hewlett-Packard, Optoelectronics Division, Palo Alto, CA 94303.

TABLE OF CONTENTS

1. INTRODUCTION

Owing to the low attenuation and dispersion of silica fibers for wavelengths in the 1.0-1.6 μm region, there has been considerable interest in the development of improved photodetectors sensitive to these wavelengths.[3-8] The InGaAsP/InP materials system seems particularly attractive for fabrication of photodiodes and avalanche photodiodes (APDs) since InGaAsP layers with bandgaps between 0.92 μm and 1.65 μm can be grown lattice matched onto high quality InP substrates.[9,10] This report is the third of a series[11,12] of interim reports describing our on-going work to develop InGaAsP APDs suitable for use in fiber optic links employing wavelengths between 1.0 and 1.3 μm.

InGaAsP APDs are quite good in many respects. We have reported[8,12] uniform rf gains up to 42 and have observed quantum efficiencies up to 70% at 1.28 μm (with no anti-reflection coating). Subnanosecond rise and fall times have also been observed, both in this laboratory and in others.[4,5] However, it has generally been found[5-8] that there is a large increase in leakage current in the avalanche gain region of bias even though the leakage current at half the breakdown voltage is very small,[8,11,12] and gain uniformity scans show no microplasmas.[4,5,8,11,12] The increased leakage current limits useful (i.e., low noise) gains to rather modest values.[8,12]

In this report we describe our recent experiments, which have clarified the nature of this increase in leakage current. In particular, we now know that the increased leakage is due to bulk properties, rather than to surface

effects as once suspected.[8,11,12] Two of the experiments are particularly forceful in indicating the bulk nature of the leakage current. In the first experiment, guard ring APDs (GRAPDs) were successfully fabricated, but the increased leakage current persisted. In the second experiment, the leakage current of a large randomly-chosen sample of APDs of different area was examined. Statistical analysis showed convincingly that the leakage current was proportional to diode area, not perimeter. Unfortunately, the cause of the increase in bulk leakage current remains unknown.

Since the leakage current in InGaAsP APDs seems to be a bulk property, future progress is hard to predict. There is some hope that the leakage current problem may be side-stepped by employing an InGaAsP absorbing region and a separate InP avalanching region. Low frequency data by K. Nishida et al[13,14] are encouraging, but so far rf gains have been reported only up to 10. Fabrication of similar structures in this laboratory is in progress.

2. EXPERIMENTS INDICATING THE BULK NATURE OF THE APD LEAKAGE CURRENT

2.1 Noise Analysis

In previous work[8,12] we have shown how the gain (M^*) associated with the leakage current may be obtained from noise measurements under the reasonable but rough approximation that the excess noise factor, F, is equal to the average photocurrent gain, M. Previously, noise data had been gathered for only one diode, so the degree to which the noise behavior was representative was unknown. To extend our earlier work, we examined the noise behavior of a set of 5 randomly-selected APDs, each having an area of 7.3×10^{-4} cm^2 and a bandgap of 1.00 eV. Noise was measured in a 10-kHz bandwidth centered at 12 MHz, using a spectrum analyzer in conjunction with a transimpedance-type preamplifier. Calibration was provided by using at the preamp input a calibrated sinusoidal current generator whose power spectrum was much narrower than 10 kHz. A comparison of M and M^* for the randomly-selected APDs is shown in Fig. 1. It is evident that $M^* \approx M$. Values of $M^* >> M$ would indicate hidden gain nonuniformities, while values of $M^* << M$ would indicate shunt leakage around the p-n junction. Since $M^* \approx M$, the large increase in leakage current must come from a correspondingly large increase in the premultiplication (primary) leakage current, rather than from any hidden gain nonuniformities. In other words, the increased leakage current seems to be associated with a strongly voltage-dependent value of the premultiplication reverse "saturation" current, rather than with microplasmas. The increase in the premultiplication leakage current is also the cause of gain saturation.[8,11,12] The cause of the increased leakage

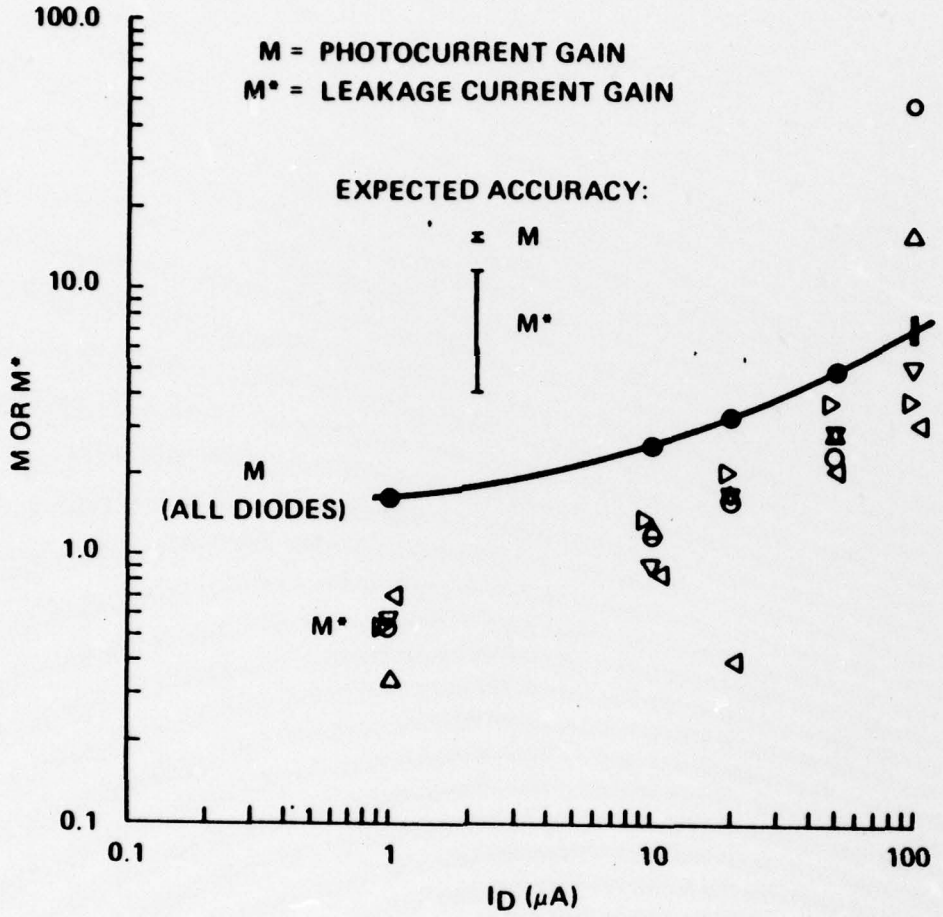

Fig. 1 Leakage current and photocurrent gain comparison for 5 randomly-selected APDs.

current is still unknown. However, as discussed below, it is apparently associated with a bulk rather than a surface effect.

2.2 Guard Ring APDs

We have observed that the leakage current in InGaAsP APDs is quite sensitive to surface treatment,[8,11,12] and hence had suspected that the leakage current was surface dominated. In an effort to reduce the leakage current, we fabricated some guard ring APDs (GRAPDs). The guard rings functioned properly but did not eliminate the increase in leakage current in the avalanche gain region, thereby indicating that the leakage current is a bulk rather than a surface problem. We now discuss these GRAPDs.

The structure of these GRAPDs is shown in Figs. 2a and 2b. The inner (active) area of our GRAPDs has a diameter of 4 mils while the outside diameter of the mesa is about 8 mils. The n-InGaAsP layer was grown by liquid phase epitaxy (LPE) and has a carrier concentration of 1-2 x $10^{16}cm^{-3}$ and a bandgap of ≈1.00 eV. The lattice match to InP is within 0.03%. The complex guard ring structure was obtained by using a top layer of p or p^+ InP, grown by vapor phase epitaxy (VPE), as a dopant source for a subsequent drive-in diffusion. The GRAPD fabrication involves two separate diffusion steps so there are two separate VPE layers involved. The first is grown selectively, using oxide masking, and serves as the dopant source (Zn) for the deep diffusion forming the ring part of the GRAPD. This layer is later removed with HCl (which does not etch InGaAsP). Later a second VPE layer of InP is grown over the entire surface of the InGaAsP and a shallow drive-in diffusion is performed, thereby forming a nearly one-sided p^+-n homojunction in the

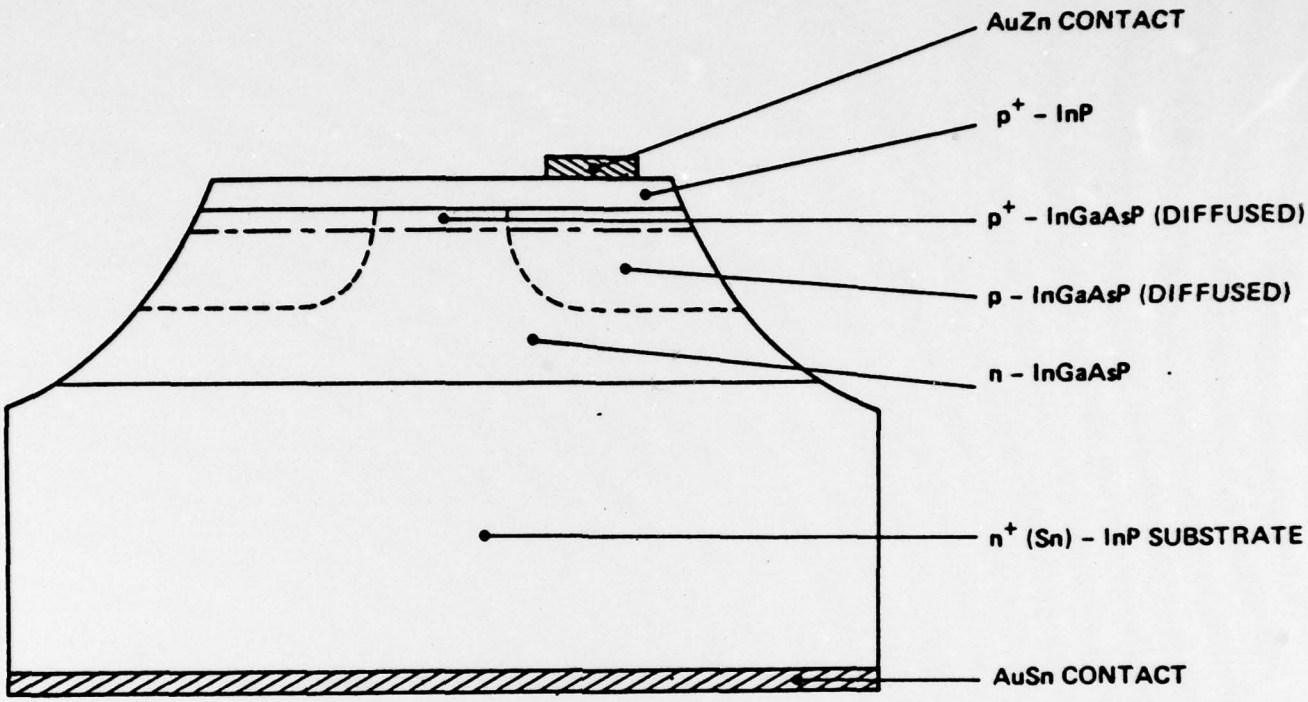

(a)

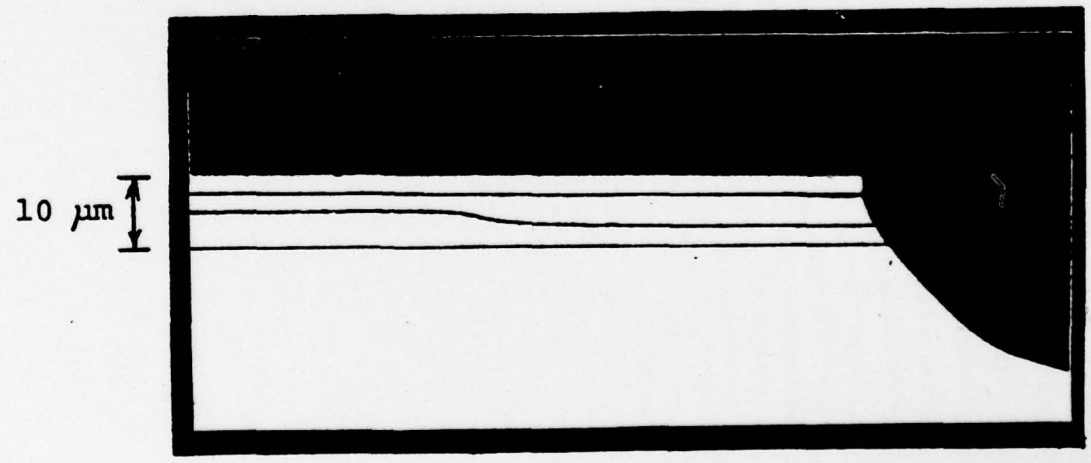

(b)

Fig. 2 Guard ring InGaAsP APD structure.

central region within the guard ring. In general, this second (shallow) diffusion is not necessary. However, submicroscopic damage has occurred during some of the previous high temperature processing steps, and the second diffusion was found to reduce the leakage current.

To substantiate that the guard rings were effectively isolating the interior region from the outer surfaces, we fabricated some 5-mil diameter mesa-structure reference diodes on the same wafer as the GRAPDs (in alternate rows). These reference diodes had junctions formed from only the (first) deep diffusion, and therefore serve to independently test for the typical breakdown voltage and leakage current of the outer ring junctions of the GRAPDs. For the wafer of Fig. 2b, the typical interior junction breakdown voltage was 15 V lower (76 V) than the typical exterior breakdown voltage (91 V). Gain uniformity scans showed that gain occurred only in the central region of the GRAPD, so that any surface leakage is not expected to be multiplied. Figures 3a and 3b show a comparison of the typical I-V characteristics of the two types of diodes. For the complete GRAPD, gains occurred mostly at the microamp level of leakage current (1 MHz gains of M = 2, 4, 10, and 25 occurred at leakage currents of 0.2, 2, 6, and 150 μA, respectively). Figure 3a shows that the voltage is 74 V when the GRAPD is operated at 2 μA of leakage current (where the gain is 4). Note from Fig. 3b, however, that the reference diode had only around 20 nA of leakage current at 74 V. This indicates that the shunt surface leakage current of the outer ring junction of the complete GRAPD is expected to be less than 100 nA at 74 V, and yet the complete GRAPD has 2 μA of leakage at 74 V and M = 4. Hence essentially all the leakage current is coming from the bulk rather than the surface.

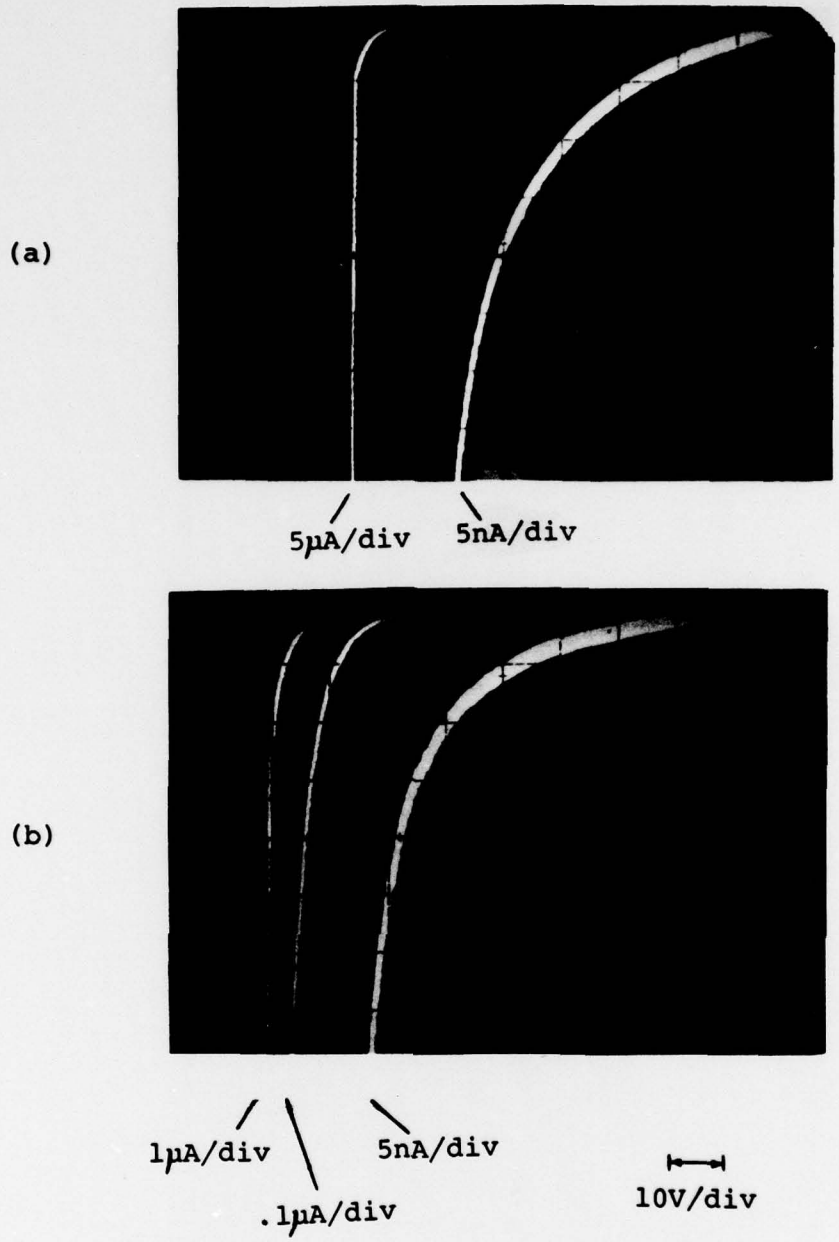

Fig. 3 APD reverse bias unilluminated I-V characteristics.

(a) Complete guard ring APD: Active diameter is 4 mils; total diameter is 8 mils.

(b) Nearby APD with ring junction only. Diameter is 5 mils. Both diodes exhibit rf gain.

2.3 Area Dependency of Leakage Current

While the GRAPD results indicate that the leakage current is a bulk, rather than a surface problem, it is still desirable to confirm this with a different and independent method. To do this, we performed a statistical analysis of the leakage current in a large sample of APDs having two different sizes. At low gains, the standard deviations were small enough to conclude with confidence that the leakage current scaled linearly with area rather than perimeter, thus indicating the bulk nature of the leakage current. This experiment is now described.

A 1.00-eV bandgap InGaAsP APD wafer was fabricated (as previously reported[8,11,12]) with two sizes of unguarded APDs located in alternate rows on the wafer. Their diameters were 14.5 ± 0.2 mils and 5.5 ± 0.2 mils. The diodes were randomly selected by going up and down rows, without skipping (either diodes or rows), on an arbitrarily-chosen region of the wafer that was approximately square-shaped. Diodes with shorts or obvious early breakdowns were rejected. Twenty-nine diodes were examined to obtain 11 good large-area APDs and 11 good small-area APDs, with six large-area diodes and one small-area diode being rejected because of shorts or early breakdown. Statistical data was obtained for each group of 11 diodes. Statistical analysis is also given for groups of 10 diodes each, with the leakiest diode of each group being omitted. This tightens up the standard deviations.

Table I summarizes the results. Leakage current and gain were measured at four different voltages. At low biases (25 V), we see that the leakage current is small but

BIAS VOLTAGE (V)	a) DIODE DIAMETER (MILS)	GAIN	b) I (μA)	RANGE OF I (μA) MIN, MAX	c) $\frac{I_{LARGE\ AREA}}{I_{SMALL\ AREA}}$	d) $\frac{I_{LARGE\ AREA}\ (\mu A)}{I_{SMALL\ AREA}\ (\mu A)}$
25.00	14.5 5.5	1 (DEF.) 1 (DEF.)	0.12 ± 0.23 0.013 ± 0.030	0.0086, 0.79 0.00025, 0.10	9.2 ± 27.7	$\frac{0.049 \pm 0.057}{0.0048 \pm 0.0071} = 10.2 \pm 19.2$
47.00	14.5 5.5	1.65 ± 0.08 1.59 ± 0.06	7.5 ± 4.6 0.91 ± 0.47	4.5, 20.2 0.6, 2.3	8.2 ± 6.6	$\frac{6.2 \pm 1.9}{0.77 \pm 0.12} = 8.1 \pm 2.8$
50.60	14.5 5.5	2.28 ± 0.15 2.18 ± 0.06	28.4 ± 9.0 3.74 ± 0.92	21, 45 3.0, 6.0	7.6 ± 3.0	$\frac{26.8 \pm 7.4}{3.51 \pm 0.56} = 7.6 \pm 2.4$
53.80	14.5 5.5	3.57 ± 0.26 3.64 ± 0.14	183 ± 139 16.7 ± 3.5	91, 522 13.8, 24.6	11.0 ± 8.6	$\frac{149 \pm 86}{15.9 \pm 2.5} = 9.4 \pm 5.6$

a) TOLERANCE IS ± 0.2 MIL. AREA RATIO IS 6.95 ± 0.54; CIRCUMFERENCE RATIO IS 2.64 ± 0.10.

b) 29 RANDOMLY SELECTED DIODES WERE EXAMINED TO GET 22 GOOD APD'S, 11 OF EACH SIZE, WITH 6 LARGE AREA AND 1 SMALL AREA DIODES BEING REJECTED AT THE OUTSET, DUE TO THE PRESENCE OF SHORTS OR PREMATURE BREAKDOWN.

c) THE STANDARD DEVIATION OF $(A \pm \sigma_A) / (B \pm \sigma_B)$ IS ASSUMED TO BE

$$\sigma_{A/B} = (A/B)\left[(\sigma_A/A)^2 + (\sigma_B/B)^2\right]^{1/2}$$

d) LEAKIEST DIODE OF EACH SIZE OMITTED.

TABLE I

Area dependence of APD leakage current.

varies wildly, having a standard deviation several times the mean value. However, for gains around 2 (47.00 V, 50.60 V), the leakage current has increased to the microamp level and does not vary too wildly, having a standard deviation only a fraction of the mean value. At still higher values of voltage (53.80 V) or gain, however, the leakage current is increasing quite rapidly and again begins to vary rather wildly. The last two columns in Table I show that the leakage current is proportional to the area, rather than to the perimeter. The most statistically significant data occur near M = 2.2, where the leakage current ratio of 7.6 ± 2.4 agrees rather well with the ratio of areas, 6.95 ± 0.54, but not with the ratio of perimeters, 2.64 ± 0.10. Hence the bulk nature of the leakage current is again indicated.

The relative standard deviations in Table I are smaller in the low gain region around M = 2, because in this region the leakage current is dominated neither by occasional defects (which dominate at low currents) nor by microplasmas (which dominate at high currents). An elaboration may be helpful:

At low leakage currents (e.g. < 100 nA) the leakage current is dominated by "occasional defects" such as dislocations, surface deposits, occasional unwanted impurities, etc. Most such defects scale with area, but when there is only a low probability of any given defect occurring on a small-area diode, the relative variations in the density of a particular type of defect between diodes can be huge (e.g., 0 vs. 1). Furthermore, one type of defect might cause little leakage current while another type might cause a large amount. On the other hand, at very large values of leakage current or gain, even extremely uniform diodes would begin to form microplasmas, although not all at exactly the

same voltage. Hence, at very large values of leakage current, one again expects the leakage current to vary wildly at a given voltage. Thus, one expects to find the most uniform distribution of leakage current in a sample of diodes at low to moderate values of gain or leakage current. In this region, the leakage current is dominated neither by occasional defects nor by microplasmas. This is why the most statistically significant data in Table I occurs near M = 2.2, where the leakage current ratio of 7.6 ± 2.4 agrees rather well with the ratio of areas, 6.95 ± 0.54, but not with the ratio of perimeters, 2.64 ± 0.10. If a gaussian distribution of probabilities is assumed, these standard deviations indicate that the probability of the leakage current being within 30% of being proportional to area is over 60%, while the probability of being within 30% of being proportional to perimeter is only 3%. Hence the bulk nature of the leakage is indicated.

Note also from Table I that the leakage current <u>variations</u> are quite small for the diodes of smaller area (1.5×10^{-4} cm^2). Hence if there is a common defect responsible for this leakage current, it must have a density greater than $10^5/cm^2$. This appears to rule out dislocations, as their density is too low. This conclusion is further supported by the similarity in yields and leakage current between unguarded APDs fabricated on dislocation-free Zn-doped substrates, and the GRAPDs fabricated on Sn-doped substrates having a dislocation density of $\sim 10^4/cm^2$. (The Zn substrates give only slightly better yields and leakage currents.)

The leakage current is not only a bulk problem, but indeed seems to be rather <u>uniform</u> bulk property. In particular, the leakage current at a given value of gain (or voltage) has little variation between different diodes from

the same wafer. If the increased leakage current was associated with the conventional type of microplasmas, this would not be the case. In a random sampling[15] of 12 APDs (from a single wafer) we found the post-multiplication leakage current density at an rf photocurrent gain of 10, was 0.25 ± 0.033 A/cm^2, for APDs of area $7.3 \times 10^{-4} cm^2$. The standard deviation represents only a 13% variation -- remarkably small. For the same random sample, the standard deviation of the breakdown voltage was also extremely small -- less than 0.5%.

We do not yet know the cause of the increase in leakage current near the breakdown voltage. However, we now know that the increased leakage is associated with a rather uniform bulk property, rather than a surface effect, and that the increased leakage does not appear to be caused by hidden gain nonuniformities.

3. OTHER WORK

3.1 An Annealing Experiment

The question arises whether high temperature annealing of previously grown InGaAsP layers might lead to increased microscopic homogeneity and thereby lead to reduction of the leakage current in the avalanche gain bias region. We tested this hypothesis and concluded that any beneficial effect was small. We now describe the experiment.

An InGaAsP layer (thickness ~8 μm, bandgap ≈ 1.00 eV, n-type doping ≈2 x 10^{16} cm^{-3}) was grown on a n^--InP substrate. Half of this wafer was annealed in an evacuated quartz ampoule at 950°C for 1 hour. An overpressure of P was present, provided by red phosphorus, and the layer side was coated with silicon nitride. After the anneal, no decomposition was observed at 400X magnification. From this point on, both halves of the original wafer were processed exactly in parallel. About 2 microns was etched off the InGaAsP layer (both halves) with 0.1% Bromine-Methanol. This is done to remove any effects the silicon nitride may have caused on the top of the quaternary layer of the annealed half. A p^+-InP layer was then grown by VPE on top of both halves. A drive-in diffusion was then performed on both pieces (1/2 hour at 850°C) to move the junction about 2 μm below the top InP layer, thus forming a p-n homojunction in the quaternary layer. This drive-in diffusion step has only a minor annealing effect on the unannealed half of the wafer (compared to 1 hour at 950°C). Such a drive-in diffusion is necessary to reduce leakage current and to prevent edge breakdown by causing a graded junction. Subsequently both halves of the wafer were fabricated into mesa geometry APDs.

Electrical and optical evaluation showed that both the annealed and unannealed pieces had similar performance; i.e., the better diodes had similar gain and similar leakage current at a given value of gain. Yields were fairly poor and this prevented a quantitative statistical analysis from being performed. Hence it is possible that small differences in quality existed between the annealed and unannealed pieces. However, any differences were small enough not to be obvious. The relatively complex procedure used for this annealing experiment was chosen in order to try to achieve an identical doping profile on both the annealed and unannealed pieces, so that a variation in doping profile would not confuse the comparison.

3.2 Antireflection Coating

Silicon nitride was tested as an antireflection coating by depositing a 1550 Å thick layer onto some in-house InGaAs photodiodes having the structure p^+-InP/p(diffused)-InGaAs/n-InGaAs/n^+-InP(substrate). These photodiodes had diameters of 15 mils, leakage currents down to $2 \times 10^{-5} A/cm^2$ at -20V, and subnanosecond rise and fall times. With the measured index of refraction of 2.0, a 1550 Å thick layer of silicon nitride is expected to have a minimum reflectivity at a wavelength of 1.24 μm. The quantum efficiency was measured at 1.22 μm using an InGaAsP LED, and a calibrated Ge reference diode. The observed quantum efficiency was nearly 100%, having the value (95 ± 5)%. Without an antireflection coating, the maximum theoretical quantum efficiency is only about 70%, so the silicon nitride coating evidently works quite well as an antireflection coating. Silicon nitride will work equally well for the InGaAsP APDs.

3.3 Junction Coatings

Until convenient hermetic packaging schemes are implemented that allow efficient coupling to optical fibers, it is desirable to have some kind of p-n junction coating that can protect exposed junctions in ordinary (not overly harsh) environments. A silicone gel junction-passivation coating from Corning was found to be unsatisfactory. When coated APDs were biased at even low voltages, the leakage current would slowly and steadily increase. The associated time constant was large (minutes) and the leakage current would eventually approach the microamp level (having started from the nanoamp level). On the other hand, a transparent epoxy from Epo-Tek worked extremely well. The low level leakage current was very stable and had not increased from its value prior to the epoxy application.

Si_3N_4 and SiO_2 are also potential junction coatings. However, relatively high temperature depositions (>>225°C) seem to be required as depositions at 225°C or less have led to very large increases in leakage current.

4. FUTURE WORK

Initially it had been intended to emphasize the design of a preamp module to use with the APDs at this stage of our contract work. However, due to the limited performance of the APDs, emphasis has remained on the APD development. We will soon shift most of our efforts toward the design of the APD + preamp module. However, first we intend to investigate the high-frequency gain and noise performance of the new type of hybrid InP APD reported by K. Nishida et al,[13,14] that employs an InP avalanche region and a separate InGaAsP absorbing region.

5. REFERENCES

1. J. Conradi, F. P. Kapron, J. C. Dyment, IEEE Trans. Electron Devices ED-25, 180 (1978).

2. T. Miya, Y. Terunuma, T. Hosaka, T. Miyashita, Electron. Lett. 15, 106 (1979).

3. H. H. Wieder, A. R. Clawson, G. E. McWilliams, Appl. Phys. Lett. 31, 468 (1977).

4. H. D. Law, L. R. Tomasetta, K. Nakano, Appl. Phys. Lett. 33, 920 (1978).

5. C. E. Hurwitz, J. J. Hsieh, Appl. Phys. Lett. 32, 487 (1978).

6. M. Feng, J. D. Oberstar, T. H. Windhorn, L. W. Cook, G. E. Stillman, B. G. Streetman, Appl. Phys. Lett. 34, 591 (1979).

7. T. P. Lee, C. A. Burrus, A. G. Dentai, J. Quantum Electron. QE-15, 30 (1979).

8. R. Yeats, S. H. Chiao, Appl. Phys. Lett. 34, 583 (1979).

9. G. A. Antypas, R. L. Moon, J. Electrochem. Soc. 120, 1574 (1973).

10. Y. Seki, H. Watanabe, J. Matsui, J. Appl. Phys. 49, 822 (1978).

11. R. Yeats, S. H. Chiao, Interim Report No. 1, "III-V Heterostructure Avalanche Photodiode Modules for Fiber Optic Communication Links in the 1.0 to 1.3 Micrometer Spectral Range," U.S. Army Communications R&D Command, Fort Monmouth, NJ, Contract DAAB07-78-C-2402, September (1978).

12. R. Yeats, S. H. Chiao, Interim Report No. 2, "III-V Heterostructure Avalanche Photodiode Modules for Fiber Optic Communication Links in the 1.0 to 1.3 Micrometer Spectral Range," U.S. Army Communications R&D Command Fort Monmouth, NJ, Contract DAAB07-78-C-2402, April (1979).

13. K. Nishida, K. Taguchi, Y. Matsumoto, Appl. Phys. Lett. 35, 251 (1979).

14. K. Taguchi, Y. Matsumoto, K. Nishida, Electron. Lett. 15, 453 (1979).

15. The sample consists of the APDs delivered to the Contractor earlier this year. These are further discussed in Sec. 4 of Ref. 12.

DISTRIBUTION LIST

Defense Documentation Center
ATTN: DDC-TCA
Cameron Station (Bldg 5)
12 Alexandria, VA 22314

Director
National Security Agency
ATTN: TDL
1 Fort George G. Meade, MD 20755

DCA Defense Comm Engrg Ctr
Code R123, Tech Library
1860 Wiehle Ave
1 Reston, VA 22090

Defense Communications Agency
Technical Library Center
Code 205 (P. A. Tolovi)
1 Wash, DC 20305

Office of Naval Research
Code 427
1 Arlington, VA 22217

GIDEP Engineering & Support Dept
TE Section
P O Box 398
1 Norco, CA 91760

Director
Naval Research Laboratory
ATTN: Code 2627
1 Wash, DC 20375

Commander
Naval Electronics Laboratory Ctr
ATTN: Library
1 San Diego, CA 92152

Cdr, Naval Surface Weapons Ctr
White Oak Laboratory
ATTN: Library, Code WX-21
1 Silver Spring, MD 20910

Commandant, Marine Corps
HQ, US Marine Corps
ATTN: Code LMC
1 Wash, DC 20380

HQ, US Marine Corps
ATTN: Code INTS
1 Wash, DC 20380

Command, Control & Communications Div
Development Center
Marine Corps Development & Educ Cdmd
1 Quantico, VA 22134

Naval Telecommunications Command
Technical Library Code 91L
4401 Massachusetts Avenue, NW
1 Wash, DC 20390

Naval Air Systems Command
Code: AIR-5332
2 Wash, DC 20360

AUL/LSE 64-285
1 Maxwell, AFB, AL 36112

Rome Air Development Center
ATTN: Documents Library (TILD)
1 Griffiss AFB, NY 13441

Air Force Geophysics Lab
L. G. Hanscom AFB
ATTN: Lib
1 Bedford, MA 01730

HQ ESD (DRI)
L.G. Hanscom AFB
1 Bedford, MA 01731

HQ, Air Force Electronic Warefare Ctr
ATTN: SURP
1 San Antonio, TX 78243

HQ, Air Force Systems Command
ATTN: DLCA
Andrews AFB
1 Wash, DC 20331

Cdr, MIRADCOM
Redstone Scientific Info Center
ATTN: Chief, Document Section
2 Redstone Arsenal, AL 35809

Commander
US Army Intelligence Center
& School
ATTN: ATSI-CD-MD
1 Fort Huachuca, AZ 85613

Commander
HQ Fort Huachuca
ATTN: Technical Reference Div
1 Fort Huachuca, AZ 85613

Commander
USASA Test & Evaluation Center
ATTN: IAD-CDR-T
1 Fort Huachuca, AZ 85613

Dir, US Army Air Mobility R&D Lab
ATTN: T. Gossett, Bldg 207-5
NASA Ames Research Center
1 Moffett field, CA 94035

HQDA (DAMO-TCE)
1 Wash, DC 20310

Deputy for Science & Technology
Office, Assist Sec Army (R&D)
1 Wash, DC 20310

HQDA (DAMA-ARP/Dr. F. D. Verderame)
1 Wash, DC 20310

Cdr, Harry Diamond Laboratories
ATTN: Library
2800 Powder Mill Road
1 Adelphi, MD 20783

Director
US Army Ballistic Research Labs
ATTN: DRXBR-LB
1 Aberdeen Proving Ground, MD 21005

Director
US Army Ballistic Research Labs
ATTN: DRXBR-CA (Dr. L. Vandekieft)
1 Aberdeen Proving Ground, MD 21005

Director
US Army Materiel Systems Analysis Acty
ATTN: DRXSY-T
1 Aberdeen Proving Ground, MD 21005

Cdr, AVRADCOM
ATTN: DRSAV-E
P O Box 209
1 St Louis, MO 63166

Commander
Picatinny Arsenal
ATTN: SARPA-ND-A-4 (Bldg 95)
1 Dover, NJ 07801

Director
Joint Comm Office (TRI-TAC)
ATTN: TT-AD (Tech Docu Cen)
1 Fort Monmouth, NJ 07703

Project Manager, REMBASS
ATTN: DRCPM-RBS
2 Fort Monmouth, NJ 07703

Project Manager, NAVCON
ATTN: DRCPM-NC-TM
Bldg 2539
1 Fort Monmouth, NJ 07703

Commander
US Army Satellite Communications Agcy
ATTN: DRCPM-SC-3
1 Fort Monmouth, NJ 07703

Cdr,US Army Research Office
ATTN: DRXRO-IP
P O Box 12211
1 Research Triangle Park, NC 27709

Cdr, US Army Tropic Test Center
ATTN: STETC-MO-A (Tech Library)
Drawer 942
1 Fort Clayton, Canal Zone 09827

Commander, DARCOM
ATTN: DRCDE
5001 Eisenhower Ave
1 Alexandria, VA 22333

Cdr, US Army Signals Warfare Lab
ATTN: DELSW-OS
Arlington Hall Station
1 Arlington, VA 22212

Commander
US Army Training & Doctrine Command
ATTN: ATCD-TEC
1 Fort Monroe, VA 23651

Director, Night Vision Laboratory
US Army Electronics R&D Command
ATTN: DELNV
1 Fort Belvoir, VA 22060

Commander
US Army ERADCOM
NV/EO Lab ATTN: Dr. R. G. Buser
1 Fort Belvoir, VA 22060

Cdr/Dir Atmospheric Sciences Laboratory
US Army Electronics Command
ATTN: DRSEL-BL-SY-S
1 White Sands Missile Range, NM 88002

Chief, Avaiation Electronics Div (SIMO)
US Army Electronics Command
ATTN: DRSEL-SI-AE, P O Box 209
1 St Louis, MO 63166

Chief
Intel Material Dev & Support Ofc
Electronic Warfare Lab, ECOM
1 Fort Meade, MD 20755

Hanscom AFB
ATTN: Dr. Eirug Davies (ESO)
Deputy for Electronic Technology
1 Bedford, MA 01730

MIT - Lincoln Laboratory
ATTN: Library (RM A-082)
P O Box 73
2 Lexington, MA 02173

NASA Scientific & Tech Info Facility
P O Box 8757
Baltimore/Washington Intl Airport
1 Baltimore, MD 21240

Advisory Group on
Electron Devices
201 Varick Street, 9th Floor
2 New York, New York 10014

Advisory Group on
Electron Devices
ATTN: Secy, Working Group D (Lasers)
201 Varick Street
2 New York, NY 10014

TACTEC
Battelle Memorial Institute
505 King Avenue
1 Columbus, OH 43201

Ketron, Inc.
ATTN: Mr. Frederick Leuppert
1400 Wilson Blvd Architect Bldg
1 Arlington, VA 22209

R. C. Hansen, Inc.
P O Box 215
1 Tarzana, CA 91356

Wright Patterson Air Force Base
ATTN: Dr. D. J. Peacock
1 AFAL/DHO, Ohio 46433

Naval Ocean Systems Center
ATTN: Dr. W. Putnam
Code 8115
1 San Diego, CA 92152

Naval Ocean Systems Center
ATTN: Dr. Steve Miller
Code 922
1 San Diego, CA 92152

Laser Diode Labs
1130 Somerset Street
New Brunswick, NJ 08901
1 (ATTN: Dr. Gill)

Rockwell International Science Center
ATTN: Dr. L. Tomasetta
1049 Camino Dos Rios
Post Office Box 1085
1 Thousand Oaks, CA 91360

Bell Telephone Laboratory
ATTN: Dr. R. Nahory
1 Holmdel, NJ 07733

RCA Laboratories
ATTN: Dr. M. Ettenberg
David Sarnoff Research Laboratories
1 Princeton, NJ 08540

University of Illinois at
Urbana-Champaign
ATTN: Dr. G. E. Stillman
Department of Electrical Engineering
1 Urbana, IL 61801

RCA Limited
ATTN: Dr. R. J. McIntyre
Trans Canada Highway
1 Ste Anne-de-Bellevue, Quebec, Canada
H9X3L3

RCA Limited
ATTN: Dr. P. Webb
Trans Canada Highway
1 Ste Anne-de-Bellevue, Quebec, Canada
H9X3L3

MIT Lincoln Laboratory
ATTN: Dr. C. Hurwitz
P. O. Box 73
1 Lexington, MA 02173

Bell-Northern Research
ATTN: Mr. Barrie Kirk
10652 Wayridge Drive
1 Gaithersburg, MD 20760

ITT-Electro-Optical Div
ATTN: Dr. A. Amith
7635 Plantation Road
1 Roanoke, VA 24019

Xerox - Electro Optical Systems
ATTN: Mr. R. Gammarino
300 North Halstead Street
1 Pasadena, CA 91107

Oregon State University
ATTN: Dr. P. K. Bhattacharya
Dept of Elect & Comp Engineering
1 Corvallis, OR 97331

Commander
US Army CORADCOM
Fort Monmouth, NJ 07703

1 ATTN: DRDCO-COM-RM-1 (Dr. L. Dworkin)
1 DRDCO-COM-RM-1 (Mr. L. Coryell)
8 DRDCO-COM-RM-1 (Ms. C. Loscoe)

Spectronics
ATTN: Dr. Harold A. Allen, Vice President
830 East Anapaho Road
1 Richardson, TX 75081

Commander
Naval Ocean Systems Center Hawaii
P. O. Box 997
ATTN: Code 5334 (Mr. George Wilkins)
1 Kailua, Hawaii 96734